ELSEVIER

Journal of Fluorine Chemistry 110 (2001) 117–122

JOURNAL OF FLUORINE CHEMISTRY

www.elsevier.com/locate/jfluchem

Crystal structures of $AgAF_6$ (A = P, As, Sb, Nb, Ta) at ambient temperatures

Kazuhiko Matsumoto[a], Rika Hagiwara[a,*], Yasuhiko Ito[a], Osamu Tamada[b]

[a]*Graduate School of Energy Science, Kyoto University, Sakyo-ku, Kyoto 606-8501, Japan*
[b]*Graduate School of Human and Environmental Study, Kyoto University, Sakyo-ku, Kyoto 606-8501, Japan*

Received 13 November 2000; accepted 28 January 2001

Abstract

Structures of $AgAF_6$ (A = Sb, Ta) have been determined by X-ray single crystal studies at ambient temperatures. $AgSbF_6$ crystallizes in space group $Ia\bar{3}$ with $a = 979.85(4)$ pm, $V = 9.4076(12) \times 10^8$ pm^3, $z = 8$, and $AgTaF_6$ crystallizes in space group $P4_2/mcm$ with $a = 499.49(4)$ pm, $c = 960.51(8)$ pm, $V = 2.3964(6) \times 10^8$ pm^3, $z = 2$. Only the crystal system and cell parameters were obtained for the isomorphic $AgNbF_6$; primitive tetragonal, $a = 497.80(10)$ pm, $b = 960.40(10)$ pm, $V = 2.3799(12) \times 10^8$ pm^3, $z = 2$. The results of the Raman spectroscopy of $AgAF_6$ support the obtained structures. The structures are discussed by comparing with that of $AgPF_6$ and $AgAsF_6$ which have recently been determined in a series of our study.

Keywords: $AgPF_6$; $AgAsF_6$; $AgSbF_6$; $AgNbF_6$; $AgTaF_6$; X-ray crystallography; Raman spectroscopy

1. Introduction

Some studies on the structures of silver hexafluorometallates $Ag(I)AF_6$ (A: pentavalent atom) are available in the literature [1–3]. However, most of the single crystal structures have not been reported until the recent structural work on $AgPF_6$ and $AgAsF_6$ by X-ray crystallography [4]. $AgPF_6$ crystallizes in space group $Fm\bar{3}m$ with $a = 755.08(7)$ pm, $V = 4.3051(12) \times 10^8$ pm^3, $z = 4$. Ag^+ and PF_6^- ions form a rock salt structure with a three-fold orientational disorder of the anion. The PF_6^- is a regular octahedron. Two F atoms, defined as F(1), in a *trans*-position are located on one of the crystal axes and the other four F atoms, defined as F(2), are located on the lines bisecting the other two crystal axes. The three-fold disorder arises by the choice of crystal axis with 1/3 atomic occupancy at each F site. $AgAsF_6$ is isostructural with $AgPF_6$; $a = 775.48(21)$ pm, $V = 4.6634(37) \times 10^8$ pm^3, $z = 4$.

It is known that the array of cations and anions in $AgAF_6$ (A = Sb, Nb, Ta) exhibits the cesium chloride type, structural variations arising from the orientations of AF_6^- [1–3]. In [1], the structures of all three $AgAF_6$ were classified into the $KNbF_6$ structure in which AF_6^- is significantly compressed along its three-fold axis forming a compressed CsCl type arrangement of the ions [5]. On the other hand, in [6], $AgNbF_6$ and $AgTaF_6$ were classified in the $KNbF_6$ structure, but $AgSbF_6$ was not. In [3], $AgAF_6$ was classified into $KSbF_6$ structure [7].

In this study, structures of $AgAF_6$ (A = Sb, Ta) at ambient temperatures were determined by X-ray diffraction single crystallography. Raman spectra were also obtained to supplement the structural information. The structure of $AgNbF_6$ was discussed only on the basis of the obtained cell parameters and Raman spectrum. Finally, the structural differences were discussed based on the anion size of $AgAF_6$ (A = P, As, Sb, Nb, Ta).

2. Results and discussions

For $AgAF_6$ (A = Sb, Ta), the structural data, positional parameters and equivalent isotropic displacement coefficients, and main interatomic distances and angles are summarized in Tables 1–3, respectively.

2.1. Crystal structures

2.1.1. $AgSbF_6$

The space group $Ia\bar{3}$ was determined by systematic extinctions. The unit cell of $AgSbF_6$ is shown in Fig. 1. This structure is different from either $KNbF_6$ [5] or $KSbF_6$

* Corresponding author. Tel.: +81-75-753-5822; fax: +81-75-753-5906.
E-mail address: hagiwara@energy.kyoto-u.ac.jp (R. Hagiwara).

0022-1139/01/$ – see front matter
PII: S0022-1139(01)00418-3

Table 1
Crystal data and refinement results for $AgAF_6$ (A = Sb, Ta)

	$AgSbF_6$ (74 pm)[a]	$AgTaF_6$ (78 pm)[a]
R_1	0.0582	0.0609
R_w	0.0667	0.0709
Crystal system	Cubic	Tetragonal
Space group	$Ia\bar{3}$	$P4_2/mcm$
a (pm)	979.85(4)	499.49(4)
c (pm)	–	960.51(8)
$V \times 10^8$ (pm^3)	9.4076(12)	2.3964(6)
z	8	4
ρ_{calc} (g cm^{-3})	4.85	5.58
μ (mm^{-1})	9.941	26.933
Crystal size (mm^3)	0.23 × 0.21 × 0.15	0.15 × 0.15 × 0.15
2θ range (°)	<60	$30 < 2\theta < 60$
Extinction coefficient × 10^{-3}	1.926	None
Refinement	Full-matrix least-square on F	Full-matrix least-square on F

[a] Radius of A(+V) [9].

type [7]. The array of cations and anions is a CsCl type with no compression. The SbF_6^- anion is a regular octahedron with the Sb–F bond lengths of 188.2(2) pm and bond angle of 90.0 ± 0.2°. The bond length is in good agreement with those reported for SbF_6^- in other compounds [8]. Four orientations of SbF_6^- octahedron occur, the unit cell being a cube containing eight SbF_6^-. This unit cell coincides with that reported by Cox [2]. The Ag atom is equivalently coordinated by six F atoms from six different SbF_6^- around it, forming a distorted octahedron. The shape is roughly described by taking the three diagonal axes out of four from a cube and connecting the ends. The thermal ellipsoid of the Ag atom is elongated towards the non-coordinating SbF_6^- ions (Fig. 2) which is facing one of its triangular faces to the Ag atom. All Ag–F distance and Ag–F–Sb bond angle are uniformly equal to 250.5(2) pm and 150.2(2)°, respectively.

2.1.2. $AgTaF_6$

The diffraction patterns of $AgTaF_6$ were typical of twinned crystals. Therefore, the intensity data of the images at the higher angle, where diffraction spots were separated, were selected to perform the structure determination.

Table 3
Bond lengths, bond angles, and coordination numbers in $AgSbF_6$ and $AgTaF_6$

$AgSbF_6$			
Bond length (pm)			
Ag–F	250.5(2)	Sb–F	188.2(2)
Bond angle (°)			
Trans F–Ag–F	180.0	*Trans* F–Sb–F	180.0
Cis F–Ag–F	108.1(1)	*Cis* F–Sb–F	90.2(1)
Cis F–Ag–F	71.9(1)	Ag–F–Sb	150.2(2)
Coordination number			
Ag–F	6		
$AgTaF_6$			
Bond length (pm)			
Ag–F(1)	291(3)	Ta–F(1)	188(2)
Ag–F(2)	246(2)	Ta–F(2)	186(3)
Bond angle (°)			
F(1)–Ta–F(1)	180.0	F(1)–Ta–F(2)	90.0(9)
F(2)–Ta–F(2)	488.8(11)	Ag–F–Ta	162.1(13)
Coordination number			
Ag–F(1)	4		
Ag–F(2)	4		

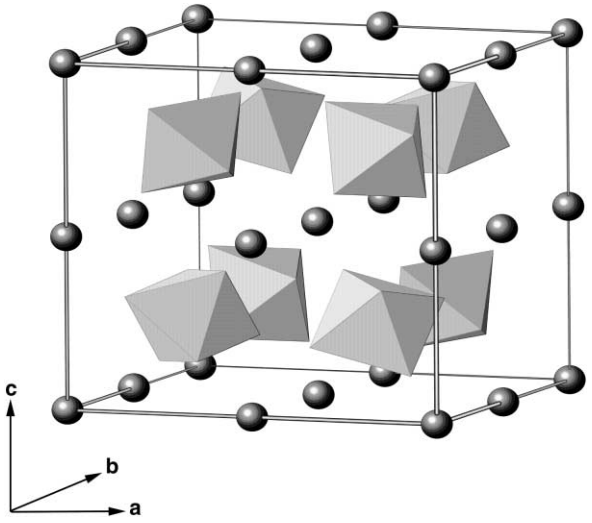

Fig. 1. The unit cell and structure of $AgSbF_6$. The origin is set at the Ag position.

Table 2
Positional parameters and equivalent isotropic displacement coefficient of $AgSbF_6$ and $AgTaF_6$

Atom	Wyckoff	Occupation	x	y	z	$U_{eq} \times 10^4$ (pm^2)
$AgSbF_6$						
Ag	8*b*	1.0	0.2500	0.2500	0.2500	0.0476(3)
Sb	8*a*	1.0	0.0000	0.0000	0.0000	0.0176(4)
F	48*e*	1.0	0.4368(2)	0.1128(2)	0.3580(2)	0.033(1)
$AgTaF_6$						
Ag	2*d*	1.0	0.5000	0.500(5)	0.250(2)	0.0310
Ta	2*a*	1.0	0.0000	0.000(5)	0.000(2)	0.0394(5)
F(1)	4*i*	1.0	0.7332	0.733(5)	0.000(2)	0.059(6)
F(2)	8*o*	1.0	0.8119	0.188(5)	0.135(2)	0.04(1)

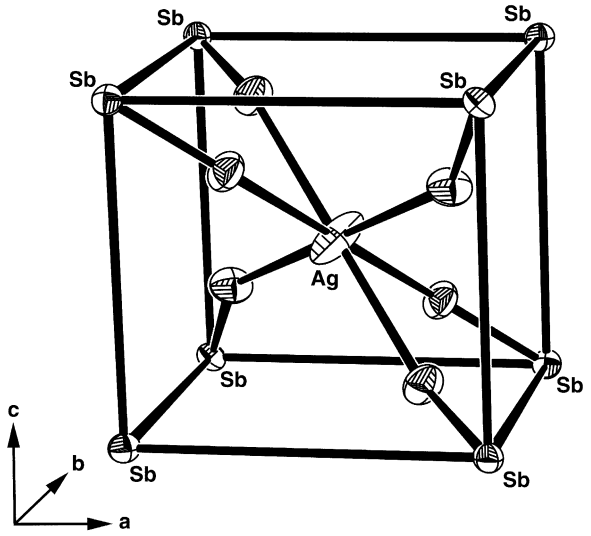

Fig. 2. The coordination of F atoms around an Ag atom.

Three space group candidates remained possible after the determination of systematic extinctions: $P4_2cm$, $P\bar{4}c2$ and $P4_2/mcm$. The structural data determined on the basis of all three space groups were very close to each other. However, when the structure of $AgTaF_6$ was solved using $P4_2cm$ or $P\bar{4}c2$ space groups, the TaF_6^- octahedron was somewhat distorted (the *cis* F–Ta–F angles are about 85°), which was not in agreement with the result of Raman spectroscopy discussed below. On the contrary, in the case of $P4_2/mcm$, the *cis* F–Ta–F angles were refined to be 88.8(11)° or 90.0(9)° giving a regular octahedron of TaF_6^-. As a result, space group $P4_2/mcm$ was selected. The unit cell of $AgTaF_6$ is shown in Fig. 3 with the cell parameters shown in Table 1. Although, the unit cell parameters are quite similar to those reported for the $KNbF_6$ structure [1], the structure differs from this structure in which K^+ and NbF_6^- form a tetragonally compressed CsCl cell [5] by a doubling of the CsCl type cell along the *c*-axis due to the different orientations of NbF_6^-. In addition, it should be noted that the shape of NbF_6^- octahedra in the $KNbF_6$ structure is significantly distorted (*cis* F–Nb–F angle is about 45°). In fact, the structure of $AgTaF_6$ is closely related to the $KSbF_6$ structure [7]. Although, the space group obtained in the case of $AgTaF_6$ ($P4_2/mcm$) is different from that in the case of $KSbF_6$ ($P\bar{4}2m$) due to the difference of the symmetry of AF_6^-, the configurations of octahedra in both the $AgTaF_6$ and $KSbF_6$ are essentially the same.

In $AgTaF_6$, an F–Ta–F axis in TaF_6^- octahedron in *trans* is parallel to the diagonal of the *ab*-plane, and the other four F atoms are placed above and below the plane at the same distance. Two staggered orientations for the TaF_6^- octahedron by the choice of the diagonals of *ab*-plane occur alternately along the *c*-axis. Fig. 4 shows the schematic illustration of the configuration of TaF_6^- octahedra along *c*-axis. The coordination number of F atoms around Ag atom is difficult to determine unambiguously, because the Ag–F

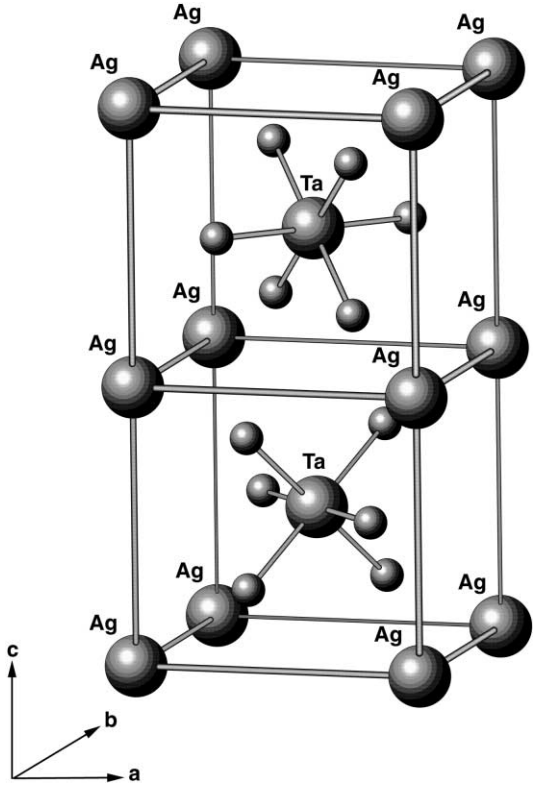

Fig. 3. The unit cell and structure of $AgTaF_6$. The origin is set at the Ag position.

distances of the first- and the second-nearest neighbors are apparently not different. The former (Ag–F(2)) is 246(2) pm, while the latter (Ag–F(1)) is 291(3), respectively. Both the coordination numbers with the nearest F atoms and the second-nearest F atoms is four, and the contribution of the coordination by the secondary neighbor should not be neglected.

2.1.3. $AgNbF_6$

X-ray diffraction single crystallography was performed on several $AgNbF_6$ crystals, but the quality of the crystals was not good enough for refinement. Only the crystal symmetry and cell parameters could be determined in the present study (Table 4). The crystal system of $AgNbF_6$ is primitive tetragonal, which is the same as that of $AgTaF_6$. The cell parameters of $AgNbF_6$ are similar to those for $AgTaF_6$ because of the similar sizes of Ta and Nb (both the ionic radii are 78 pm [9]). The Raman spectrum of $AgNbF_6$

Table 4
Some lattice parameters of $AgNbF_6$

Crystal system	Primitive tetragonal
a (pm)	497.80(10)
c (pm)	960.40(10)
$V \times 10^8$ (pm^3)	2.3799(12)
z	2

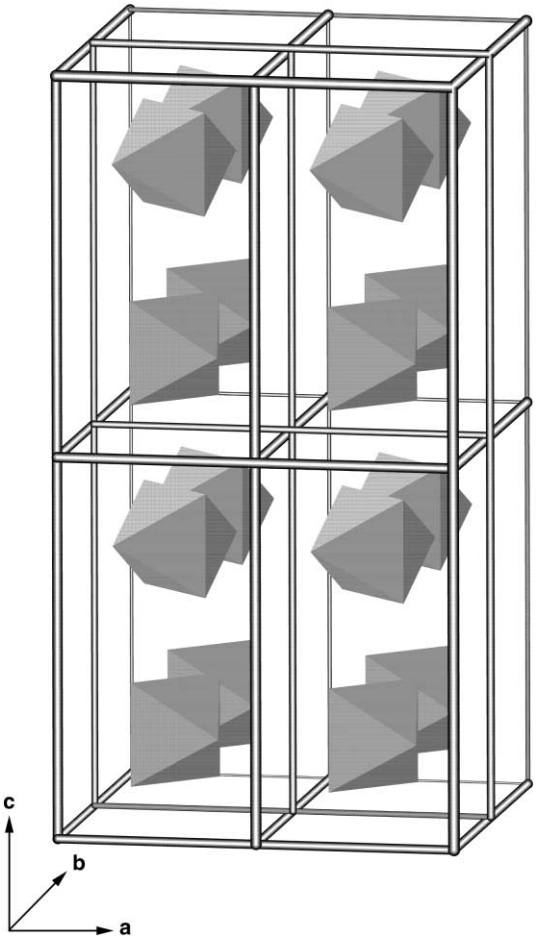

Fig. 4. Schematic illustration of the configuration of TaF_6^- octahedra in $AgTaF_5$.

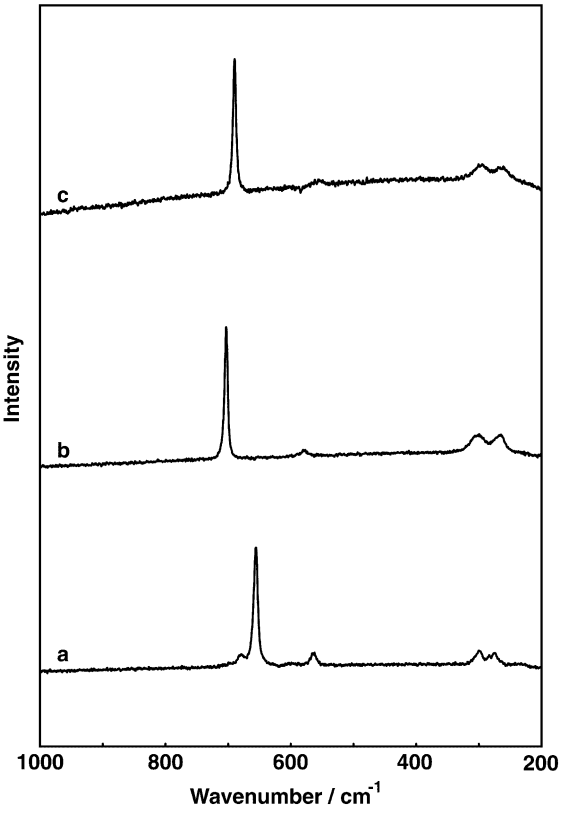

Fig. 5. The Raman spectra of: (a) $AgSbF_6$; (b) $AgTaF_6$; (c) $AgNbF_6$.

is also similar to that of $AgTaF_6$ as will be discussed below. Taking account of these similarities between $AgNbF_6$ and $AgTaF_6$, $AgNbF_6$ is probably isostructural with $AgTaF_6$ or has a very closely related structure.

2.2. Raman spectra

The results of Raman spectroscopy of $AgAF_6$ are shown in Fig. 5. The peaks assigned as fundamental modes of octahedral AF_6^-, ν_1, ν_2, and ν_5 were observed in all the spectra. The spectrum of $AgSbF_6$ (Fig. 5a) is somewhat different from that of $AgTaF_6$ (Fig. 5b) and $AgNbF_6$ (Fig. 5c). The strong ν_1 peak found at 655 cm^{-1} is accompanied by a weak broad peak at about 680 cm^{-1}. Since the single ν_1 mode is observed at 660 cm^{-1} in $KSbF_6$ for example [10], one of the possibilities is a split of the ν_1 mode. The ν_2 mode was observed at 562 cm^{-1}, which is almost the same as reported [11]. Three peaks were observed between 270 and 310 cm^{-1}. According to the structure obtained by X-ray crystallography, the site symmetry of the Sb position is S_6. Therefore, two peaks would arise from the break of the degenerate $\nu_5(F_{2g})$ mode of an O_h molecule. The possible assignment of the rest is ascribed to the difference band, $\nu_2 - \nu_5$. In the spectrum of $AgTaF_6$ (Fig. 5b), the $\nu_1(A_{1g})$ and $\nu_2(E_g)$ modes were observed at 703 and 580 cm^{-1}, respectively. The ν_5 mode was split clearly into two peaks at 300 and 265 cm^{-1}, which arise from the similar reason for the peak split as in the case of $AgSbF_6$, namely the lower symmetry D_{2h} at the Ta position in $AgTaF_6$. The Raman spectrum of $AgNbF_6$ was very similar to the spectrum of $AgTaF_6$. The ν_1 and ν_2 fundamental modes were observed at 690 and 556 cm^{-1}, respectively, while the ν_5 mode also split into two peaks at 295 and 261 cm^{-1}, which would be explained by the same reason as in the case of $AgTaF_6$.

2.3. Structural changes in $AgAF_6$ series ($A = P, As, Sb, Nb, Ta$)

The structural parameters of $AgPF_6$ and $AgAsF_6$ are summarized in Table 5 [4]. $AgPF_6$ and $AgAsF_6$ have the NaCl type array of cation and anion, whereas $AgSbF_6$, $AgTaF_6$, and $AgNbF_6$ have the CsCl type. This difference is explained by the difference of the size of anions. Concerning the structures of $M^+(AF_6)^-$, where M is a univalent atom and A is a pentavalent atom, there is a tendency as in the case of alkaline halides that the array of cations and anions favors NaCl type for small M^+ and CsCl type for large M^+ [1–3,6]. $NaAF_6$ compounds mostly crystallize in the NaCl type, whereas KAF_6 take a CsCl type array of the

Table 5
The structural parameters of $AgAF_6$ (A = P, As) [4]

	$AgPF_6$ (52 pm)[a]	$AgAsF_6$ (60 pm)[a]
Lattice constant (pm)	755.08(7)	775.48(21)
A–F bond length (pm)	F(1) 156(5) F(2) 159(3)	F(1) 166(4) F(2) 169(2)
F–A–F bond angle (°)	90	90
Averaged CN of F around Ag	10 F(1) 2 F(2) 8	10 F(1) 2 F(2) 8
Ag–F distance (pm)	F(1) 222(5) F(2) 288(3)	F(1) 222(5) F(2) 294(3)

[a] Radius of A(+V) [9].

ions. The size of the Ag^+ cation is just between these two cations and seems to take the array of the ions depending on the size of the anions. Although, both $AgSbF_6$ and $AgTaF_6$ belong to CsCl type, structural difference was observed due to the orientation of anions. It is possible that the cubic–tetragonal phase transition occurs by a small temperature difference.

The average coordination number of F atoms around Ag atom in $AgPF_6$ and $AgAsF_6$ is 10 [4], while in the case of $AgSbF_6$ the coordination number is six. As stated above, the coordination number in $AgTaF_6$, crystallographically speaking, is four but the contribution of the secondary neighbor is not neglected. Anyway, there seems to be a tendency that the coordination number of F atoms around Ag decreases as the anion size increases. In order to verify this tendency, it is necessary to check the potassium and silver salts with larger anions whose structure have not yet been determined unambiguously.

3. Experimental

3.1. General experimental procedures

The reactions were mainly performed in FEP (fluoroethylene–propylene copolymer) containers connected to a vacuum line made of SUS316 stainless steel. Solids used in this study were handled in a glove box under a rigorously dried and deoxygenated argon atmosphere. Raman spectra of powdered samples sealed in quartz capillaries (5 mm i.d.) were obtained at ambient temperatures by a BIO-RAD FTS-175C spectrometer using a Nd:YAG laser, with power of 600–1000 mW.

3.2. Synthesis and crystal growth

HF (Daikin Industries, purity > 99%) was dried over K_2NiF_6 (Ozark-Mahoning). AgF (Nacalai Tesque) was used after dissolving in HF and recrystallization to eliminate oxide impurities. $AgAF_6$ (A = Nb, Sb, Ta) were prepared by the reaction of AgF with excess SbF_5 (PCR, purity = 97%), NbF_5 (Ozark-Mahoning) and TaF_5 (Ozark-Mahoning) in HF. Using a T-shaped FEP tube, a saturated solution of $AgAF_6$ was prepared at one end of the tube and then decanted into the other end. Single crystal growth was performed at ambient temperatures by eliminating HF very slowly from the solution by cooling one end of the tube by water. Slow elimination of HF controlled by a valve was also successful to grow crystals. In a few days, single crystals were formed on the wall of the tube. After the residual solution was decanted back to the first end, HF was evacuated through a soda lime trap by a vacuum pump. By monitoring by a microscope equipped with a CCD camera, the single crystals were recovered in the argon atmosphere. A selected crystal was transferred and immobilized in the pre-sealed narrower end of a quartz capillary.

3.3. X-ray crystallographic procedures

The sealed capillary was fixed on a brass pin with adhesive to mount on a goniometer head. The data was collected at ambient temperatures using a Nonius KappaCCD diffractometer with a CCD detector and an anode using monochromated Mo Kα radiation. The power output was controlled in the range of 20–40 mA at a fixed voltage of 50 kV. The distance of the crystal to the detector was kept at 25 mm. The obtained CCD diffraction images were processed by using a graphical image processor DENZO-SMN [12]. The maXus [13] was used for determination and refinement of the structures, and the SORTAV [14] was used for absorption correction. Final refinement was performed by introducing anisotropic thermal parameters for all the atoms. Crystallographic data for the structures in this paper have been deposited with the Fachinformationzentrum Karlsruhe (FIZ) as supplementary publication nos. CSD 411795 and CSD 411796. Copies of the data can be obtained, free of charge, on application to FIZ, abt. PROKA, 76344 Eggenstein-Leopoldshafen, Germany (Tel.: +49-7247-808-205; e-mail: crysdata@fiz-karlsruhe.de).

References

[1] R.D.W. Kemmitt, D.R. Russell, D.W.A. Sharp, J. Chem. Soc. (1963) 4408–4413.
[2] B. Cox, J. Chem. Soc. (1956) 876–878.
[3] A.F. Wells, Structural Inorganic Chemistry, 5th Edition, Clarendon Press, Oxford, 1984, pp. 456–458.
[4] K. Kitashita, R. Hagiwara, Y. Ito, O. Tamada, Solid State Sci. 2 (2000) 237–241.
[5] H. Bode, H.V. Döhren, Acta Cryst. 11 (1958) 80–82.
[6] D. Babel, Structural chemistry of octahedral fluorocomplexes of the transition elements, in: C.K. Jorgensen, J.B. Neilands, R.S. Nyholm, D. Reinen, R.J.P. Williams (Eds.), Structure and Bonding, Vol. 3, Springer, New York, 1967, pp. 5–12.
[7] G.J. Kruger, C.W.F.T. Pistorius, A.M. Heyns, Acta Cryst. B32 (1976) 2916–2918.
[8] B.A. Fir, M. Gerken, B.E. Pointner, H.P.A. Mercier, D.A. Dixon, G.J. Schrobilgen, J. Fluorine Chem. 105 (2000) 159–167.

[9] R.D. Shannon, Acta Cryst. A32 (1976) 751–767.
[10] A.I. Popov, A.V. Scharabarin, V.F. Sukhoverkhov, N.A. Tchumaevsky, Z. Anorg. Allg. Chem. 576 (1989) 242–254.
[11] K. Nakamoto, Infrared and Raman Spectra of Inorganic and Coordination Compounds. Part A. Theory and Applications in Inorganic Chemistry, 5th Edition, Wiley/Interscience, 1997, pp. 216–218.
[12] Z. Otwinowski, W. Minor, Processing of X-ray diffraction data collected in oscillation mode, in: C.W. Carter Jr., R.M. Sweet (Eds.), Methods in Enzymology, Vol. 276, Academic Press, New York, 1997, pp. 307–326.
[13] S. Mackay, C.J. Gilmore, C. Edwards, N. Stewart, K. Shankland, maXus Computer Program for the Solution and Refinement of Crystal Structures, Nonius, MacScience, The University of Glasgow, Glasgow, 1999.
[14] R.H. Blessing, Acta Cryst. A51 (1995) 33–38.